Journal of Agricultural Chemistry and Environment, 2025, 14(3), 359-376
https://www.scirp.org/journal/jacen
ISSN Online: 2325-744X
ISSN Print: 2325-7458

Quantitative Mapping of Soil Erosion Using GIS/RUSLE Approach in the Falémé Sub-Watershed (Senegal/Kédougou)

Adama Ndiaye[1*], Khady Mame Diarra Sene[1], Macoumba Loum[1], Elhadji Faye[2]

[1]National Institute of Pedology (INP), Soil Science Research Laboratory, Dakar, Senegal
[2]Forest Production Department, High Institute of Agricultural and Rural Training (ISFAR), Alioune Diop University (UAD), Bambey, Senegal
Email: *adamandiaye88@gmail.com

How to cite this paper: Ndiaye, A., Sene, K.M.D., Loum, M. and Faye, E. (2025) Quantitative Mapping of Soil Erosion Using GIS/RUSLE Approach in the Falémé Sub-Watershed (Senegal/Kédougou). *Journal of Agricultural Chemistry and Environment*, **14**, 359-376.
https://doi.org/10.4236/jacen.2025.143025

Received: May 7, 2025
Accepted: August 9, 2025
Published: August 12, 2025

Abstract

The Faleme sub-watershed is influenced by several environmental factors. Located at the convergence of the Sudano-Guinean, Sudanian, and Sahelian climatic zones, the region is subject to diverse rainfall regimes. It is also an area of intense economic activity, notably mining and agriculture, both of which significantly contribute to land degradation. This degradation, primarily associated with rainfall variability and the shifting course of the Falémé River, results from a combination of natural and anthropogenic factors that shape the landscape. Key influencing variables include topography, pedology, rainfall, vegetation cover, and human-induced pressure. These elements collectively exacerbate the sub-watershed's vulnerability to water-induced soil erosion, which manifests in three main forms: sheet erosion, rill erosion, and bank undercutting. The integration of remote sensing and Geographic Information Systems (GIS), combined with empirical modeling tools like RUSLE (Revised Universal Soil Loss Equation), enabled the quantification of annual soil losses. Spatial analysis and mapping revealed the most erosion-prone areas, particularly in the southern section, where moderate to severe losses represent approximately 14% of the basin's surface area. A classification of annual soil loss levels indicated that 80.12% of the sub-watershed area falls within a tolerable range, whereas about 5% of the area experiences low losses.

Keywords

Water Erosion, Soil Loss, Index, Mining, Degradation, Modeling

1. Introduction

Soil erosion, regarded as the primary driver of land degradation, poses a serious threat to environmental integrity and human activities. When triggered by water runoff, it is referred to as water erosion, a process in which soil particles are detached and transported from upstream to downstream. Globally, this natural phenomenon results in the loss of approximately 25 billion tons of soil annually. According to the soil loss between 0.90 and 0.95 mm of topsoil each year [1]. Erosion is driven by multiple causes, and its impacts have become a major concern due to the degradation of soil quality and fertility, ultimately reducing arable land [2]. This makes erosion a significant impediment to agricultural productivity. In Sub-Saharan Africa, 494 million hectares of land are affected by soil degradation, with 46% directly attributed to water erosion. Additionally, 38% results from wind erosion, 12% from chemical degradation, and 4% from physical degradation [1]. Globally, water erosion remains the most widespread form of soil degradation. In Senegal, water erosion affects about 1.5 million hectares of arable land, especially in the central and eastern regions as well as parts of Casamance [3], where pluvial erosion is particularly severe.

Soil erosion by water arises from the interplay of various factors specific to each environment, such as rainfall, lithology, topography, vegetation cover, and human activities [4]. These factors contribute significantly to land vulnerability. A comprehensive understanding of these parameters is essential for land protection and erosion mitigation. This knowledge enables the development of the best management practices tailored to specific contexts [5] and facilitates the quantification of soil losses through various assessment and characterization methods. The methodology developed by Wischmeier & Smith (1978) remains the most widely used approach for global soil loss assessment [6].

In Africa, numerous locally adapted models have been developed to estimate water erosion, notably those informed by the work of Roose [5]. However, the physical and bathymetric assessment of erosion processes remains resource-intensive and time-consuming an obstacle for many states. Advances in Earth observation data and GIS technologies now provide cost-effective means for mapping, quantifying, and monitoring erosion prone areas [7]. This study aims to contribute to this effort by characterizing water-induced soil erosion in the Faleme sub-watershed, part of the sediment transport system of the Senegal River. This area is increasingly affected by land-use pressures, such as deforestation, farming, and artisanal mining, which weaken the soil structure and intensify erosion processes. The general objective of this study is to conduct a comprehensive assessment of water erosion and its driving factors in the study area. This includes a physical characterization of the environment, a typological study of erosion forms, and the quantification and spatial distribution of soil losses. Ultimately, this constitutes both a qualitative and quantitative characterization of soil erosion. The findings will enhance our understanding of the sub-watershed's response to water erosion within the broader hydrological context of the Senegal River basin and will help identify vulnerable areas for the implementation of targeted land conservation and restoration strategies.

2. Materials and Methods

2.1. Study Area

Located between latitudes 12˚11' and 14˚27' North and longitudes 11˚12' and 12˚15' West (**Figure 1**), the Falémé sub-basin spans three countries: Senegal, Mali, and Guinea. It covers a total estimated area of 29,927 km^2, distributed as follows: 47.8% in Mali, 39.7% in Senegal, and 12.5% in the Republic of Guinea [8]. As the main left-bank tributary of the Senegal River, the Falémé stretches for 625 km [9], originating at approximately 800 m altitude in the region of the sandstone plateau at the base of the Fouta-Djalon. It follows a regular south-to-north course and flows into the Senegal River 50 km upstream, specifically in the Bakel department. At this location, its annual flow can reach 175 m^3/s. The river is divided into three natural regions: Lower Falémé, Middle Falémé, and Upper Falémé, crossing three climatic zones: the Guinean-Sudanian zone (where it originates), the Sudanian zone, and the Sahelian zone upstream.

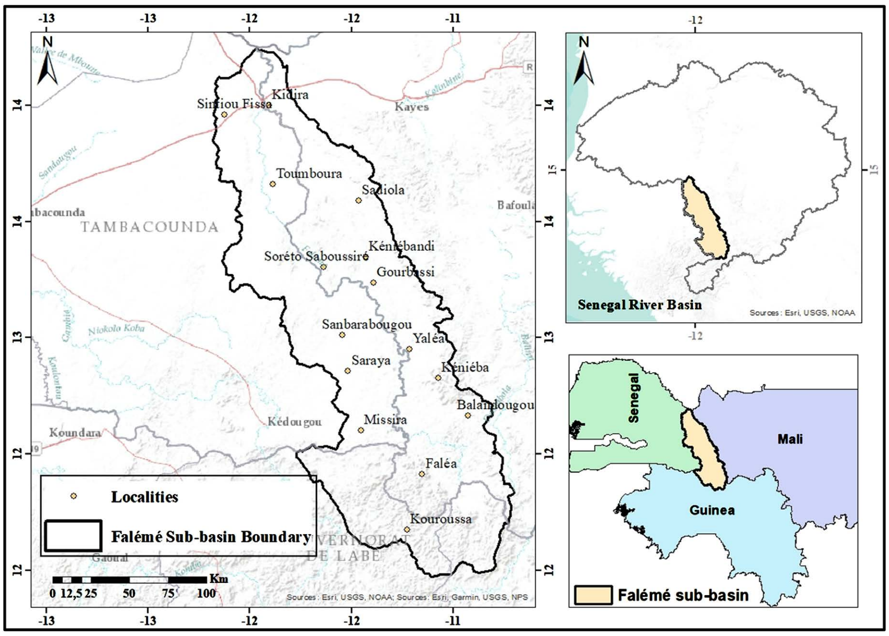

Figure 1. Geographical location of the Falémé sub-basin.

2.2. Soil Loss Quantification Using the RUSLE Method via GIS Topographic Factor LS

To quantify soil losses caused by water erosion in the Falémé sub-basin, the methodology adopted is based on the Revised Universal Soil Loss Equation (RUSLE), combined with Geographic Information Systems (GIS) and applied through the Google Earth Engine (GEE) platform. This empirical approach integrates a set of data related to soil characteristics or directly influencing factors, this allowing the analysis of erosion drivers and the prediction of potential losses.

The analysis highlights multiple factors to determine soil susceptibility to water erosion. The RUSLE method, when combined with GIS, serves as an effective tool for the spatial modeling of water erosion phenomena. Data processing is mainly carried out on Google Earth Engine, which enables task automation and facilitates large-scale analysis. According to this model, soil erosion is determined by a multiplicative function of the following factors (**Figure 2**), combined in the following Equation (A), expressed in tons per hectare per year (t/ha/year): **A = R * K * LS * C * P**.

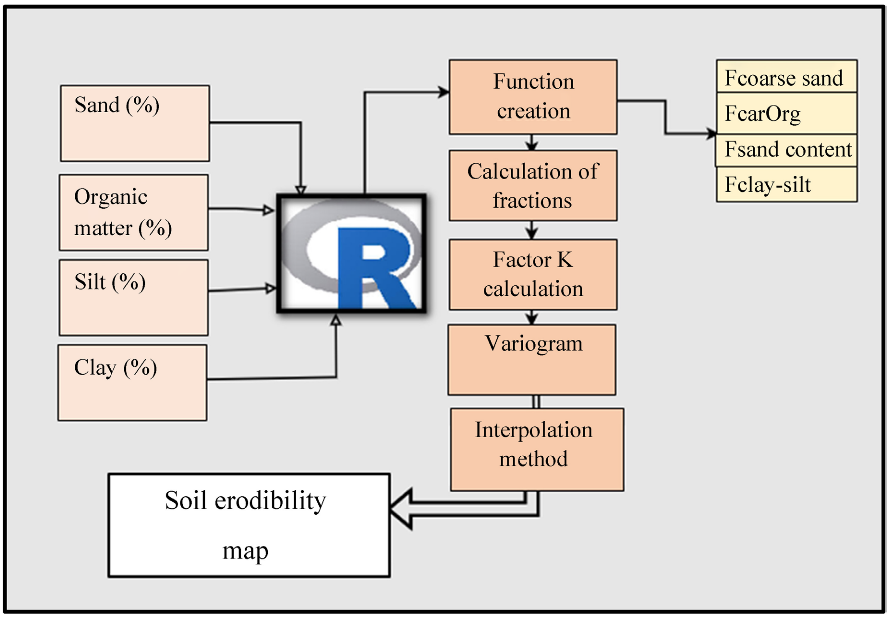

Figure 2. Workflow for computing the K factor.

2.3. Factor R

The rainfall erosivity factor **R** (MJ·mm/ha·h·year) analyzes the impact of rainfall power on soil by combining rainfall cinetic energy and maximum 30-minute intensity, following the Wischmeier & Smith [6] equation. Due to data scarcity in some regions, alternative methods have been developed, such as Roose [10] in West Africa and Nguyen [11] & Arnoldus [12], among others.

R was calculated as follows: **R = 0.548257 * P − 59.9**.

where:

R = rainfall erosivity factor (MJ·mm/ha·h·year).

P = annual precipitation (mm).

Nguyen [11] suggests using data over 54 years based on 253 weather stations [13]. For **R** calculation, CHIRPS data from 1981 to 2023 were used to capture rainfall extremes.

2.4. Factor K

The soil erodibility factor K (t·ha·h/ha·MJ·mm) is assessed based on soil structure, texture, particle size, permeability, and organic matter content [6]. In this study, the equation is applied due to data availability and its simplicity, focusing on particle size and organic matter [14].

$$K = Coarse\ Sand * ClaySilt * Org\ Matter * Sand\ Content$$

- Coarse Sand lowers K in soils with high coarse sand content.
- ClaySilt represents K in soils with high clay and silt content.
- Org Matter reduces K in soils with high organic matter.
- Sand Content decreases K in very sandy soils.

These fractions are calculated to highlight or reduce the impact of soil minerals, following Williams' (1995) formulation [14]. R programming was used to compute the fractions, and K was spatialized using Inverse Distance Weighting (IDW) interpolation. The workflow is shown in **Figure 2**.

2.5. Topographic Factor LS

The topographic factor LS (dimensionless) reflects slope length and steepness to assess their effect on erosion. It compares soil loss between two parcels with identical characteristics, differing only in slope [15]. It is closely related to slope: the steeper and longer it is, the greater the erosion risk. The equation used in this study is from [16], considering flow accumulation, image resolution, and slope:

LS = Topographic Factor.

FA = Flow Accumulation.

RS = DEM Spatial Resolution.

S = Slope.

Data processing was done on Google Earth Engine using the Hydro SHEDS collection, which offers global flow accumulation and a 30 m resolution DEM.

2.6. Factor C

The cover management factor C is crucial as it represents vegetation cover and agricultural practices' impact on erosion. It is commonly calculated using the Normalized Difference Vegetation Index (NDVI), derived from Red and Near-Infrared (NIR) reflectance:

$$NDVI = (NIR - RED)/(NIR + RED)$$

$$C = ((-NDVI + 1)/2)$$

- **NIR** = Near Infrared.
- **RED** = Red Band.
- **C** ranges from 0 to 1, with higher values indicating bare soil and lower values indicating dense vegetation that protects against erosion.

2.7. Factor P

The support practice factor P reflects human efforts to mitigate erosion. Since data are often unavailable, P is estimated using land cover and slope data. Land cover informs vegetation density, which plays a key role in soil protection. In this study, the P factor was evaluated by using land cover data combined with slope steepness, to better understand the protective measures implemented in steep areas. The "LC_Type1" band from the MODIS "Land Cover Type" collection was used for the land cover analysis, and the slope was converted into percentage.

2.8. Summary of Methodology

The set of tools and methodologies presented enabled the analysis and processing of the data necessary to obtain the results of this study. Today, data acquisition and processing are facilitated by the many technologies and techniques offered by the geospatial field (Figure 3).

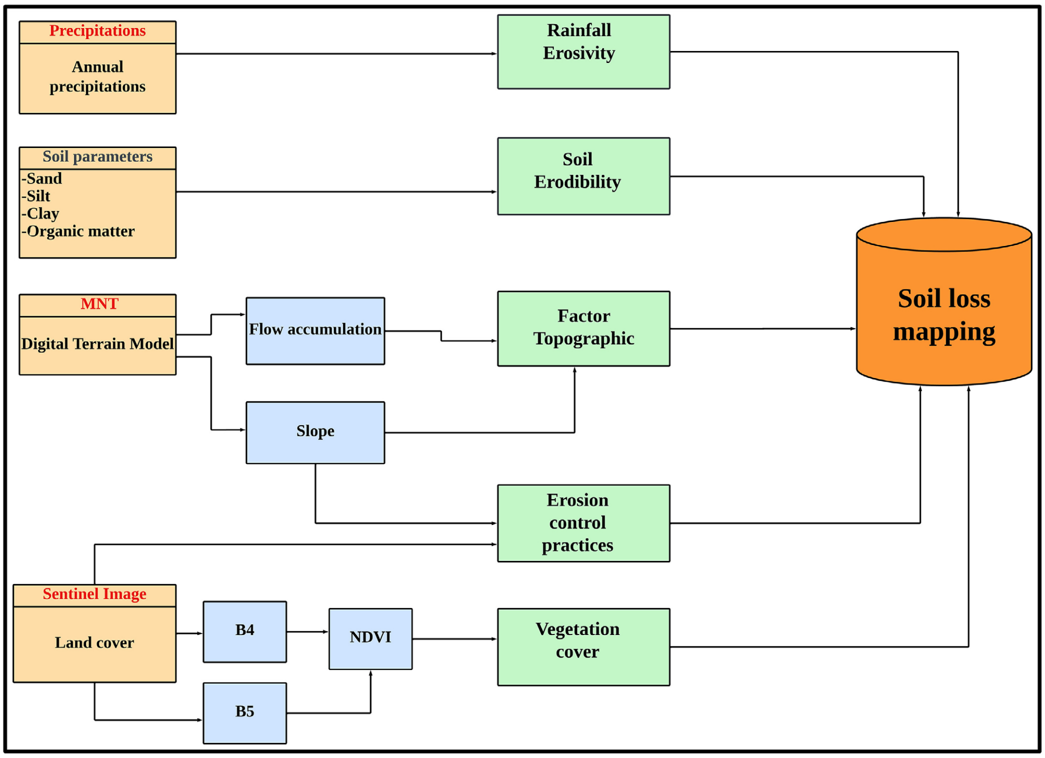

Figure 3. Workflow for annual soil loss quantification using RUSLE and GIS.

3. Data Processing and Analysis Techniques

GIS tools were essential in this study for data processing and result dissemination via mapping. The main GIS software used were ArcGIS, Google Earth Engine and QGIS.

3.1. SRTM Digital Elevation Model (DEM)

NASA's Shuttle Radar Topography Mission (SRTM) provided 30 m resolution elevation data covering over 80% of Earth's land surface, used for topographical analyses.

3.2 CHIRPS Data

Rainfall data came from the Climate Hazards Group InfraRed Precipitation with Station (CHIRPS), which combines satellite and station observations. CHIRPS data are available daily, pentad, and decadal from 1981 to present, covering latitudes 50˚ N to 50˚ S. Version 2.0 via GEE was used to calculate the R factor and conduct rainfall analysis.

3.3. MODIS Data

Moderate Resolution Imaging Spectroradiometer (MODIS) data, based on supervised classification from Terra and Aqua satellites, provide global land cover information. MODIS LC_Type1 band (500 m resolution) was used to calculate the P factor. This band is based on the IGBP land cover classification.

3.4. Sentinel-2 Satellite Images

Sentinel-2 imagery from the Copernicus program of the European Commission and ESA, was used to compute the C factor related to land cover. The 10 m resolution bands 8 (NIR) and 4 (Red) were used to calculate NDVI and assess vegetation coverage.

3.5. Soil Analysis Data

Soil laboratory analyses determined physical, chemical, and biological soil properties. These were essential for calculating the K factor. Particle size distribution (granulometry) helps define soil texture (clay, silt, sand). At INP, laser granulometry, based on light diffraction, was used. Suspended particles scatter laser light; the distribution is measured via photodiodes and interpreted using Fraunhofer theory. These parameters are vital for soil classification and inform on permeability and texture, which influence susceptibility to water and wind erosion.

4. Results and Discussion

4.1. Results

4.1.1 Soil Loss Mapping

Rainfall Erosivity (R Factor)

A key parameter in assessing rainfall aggressiveness, the R factor reflects the power with which rainfall contributes to soil degradation. The stronger and more prolonged the rainfall, the more likely it is to dislodge soil particles. This variation in the R factor, studied as a function of precipitation, follows a perfect linear relationship: for every one-unit increase in P (precipitation), the R factor increases by 0.5483. This indicates a strong dependence of rainfall erosivity on precipitation amount. The higher the precipitation (P), the higher the R value, with a maximum erosivity of 827.642 MJ/mm/ha/h/year recorded in the sub-basin (**Figure 4**).

In the Faleme sub-basin, the southern zone, known for its heavy and prolonged rainfall, is naturally the most affected area. Consequently, greater rainfall erosivity was noted in the southern part of the sub-basin compared to the north, where a minimum of 144.365 MJ/mm/ha/h/year was recorded.

Soil Erodibility (K Factor)

The soil erodibility factor (K) was studied based on pedological data from 86 samples collected throughout the sub-basin. These samples were used to analyze key soil components such as the percentages of sand, clay, silt, and organic matter. The spatialization of results was done using the Inverse Distance Weighting (IDW) interpolation method, as illustrated in **Figure 5**.

The K factor variation in the Falémé sub-basin ranges between 0.13 and 0.14 for 43.6% of the area (**Table 1**). According to the classification established by [17], as shown in (**Table 2**) most of the soils in the sub-basin are resistant to water erosion.

According to this classification, the soils in the Falémé sub-basin show notable resistance to water erosion. However, this resistance varies depending on soil type, whether sandy, clayey, or hydromorphic as the degradation and particle transport processes differ according to their specific properties.

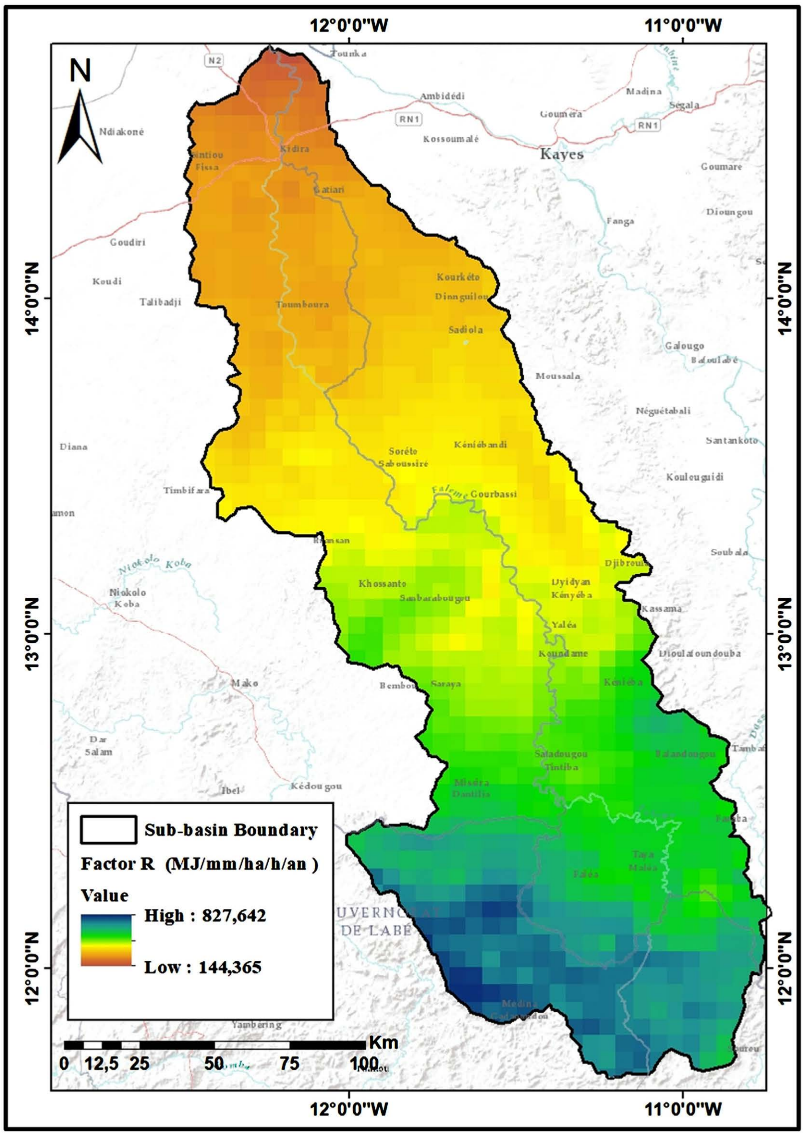

Figure 4. Rainfall erosivity factor (R) in the Falémé sub-basin.

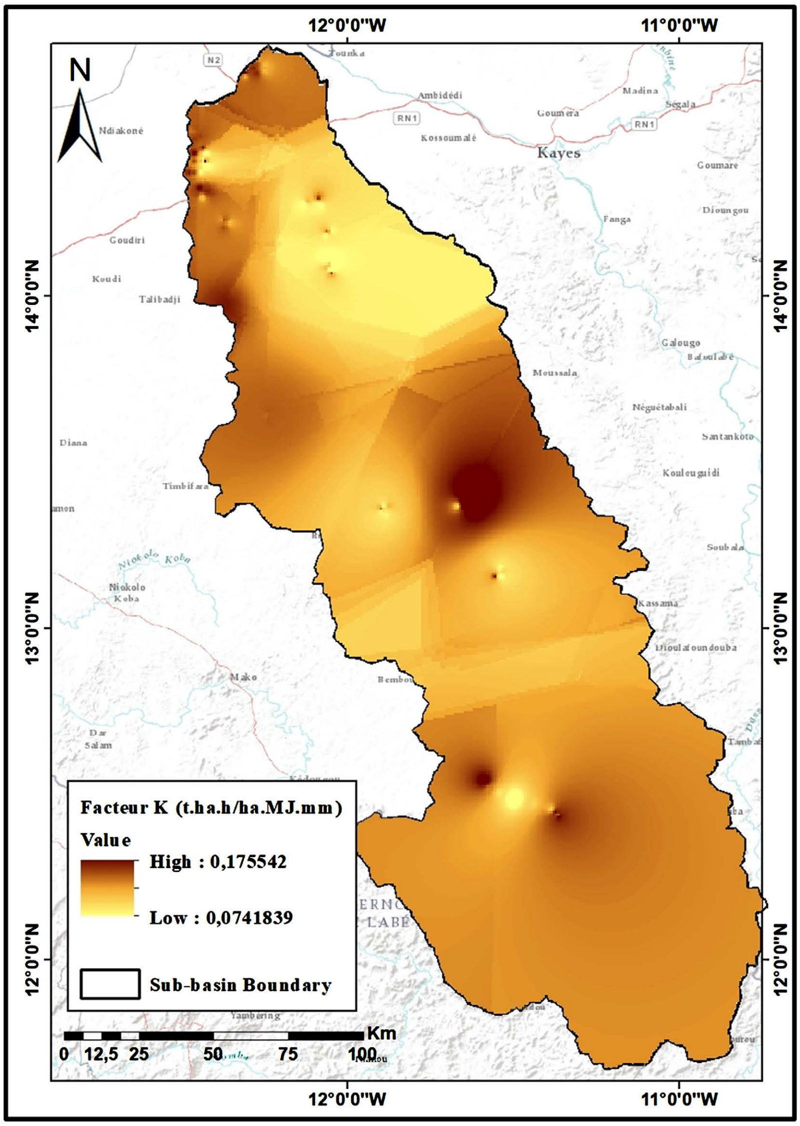

Figure 5. Soil erodibility in the Falémé sub-basin.

Table 1. Surface area (%) by soil erodibility

Classes (K)	Area (km^2)	Area (%)
0.07 - 0.12	3326.39	11.135
0.12 - 0.13	6655.88	22.281
0.13 - 0.14	13041.60	43.65
0.14 - 0.15	5828.05	19.5
0.15 - 0.17	1020.75	3.41
No data	0.41	0.001

Topographic Effect (LS Factor)

The topographic factor is a fundamental element in modeling water erosion. The use of a Digital Elevation Model (DEM) helped highlight slope steepness and length. The slope length also plays a crucial role in topographic characterization.

It is derived from flow direction and has been used to identify channels where flow is most intense, particularly along the Falémé River. As one descends downstream, the accumulation of flows becomes increasingly significant. The LS factor ranges from 0 to 46 (**Figure 6**), with the highest values found in high-altitude areas and along the banks of the main river.

Table 2. Soil classification based on erodibility [17].

Recorded K	Conclusion
K < 0.10	Erosion-resistant soil
0.10 - 0.25	Fairly resistant soil
0.25 - 0.35	Moderately sensitive soil
0.35 - 0.45	Fairly sensitive soil
>0.45	Highly sensitive soil

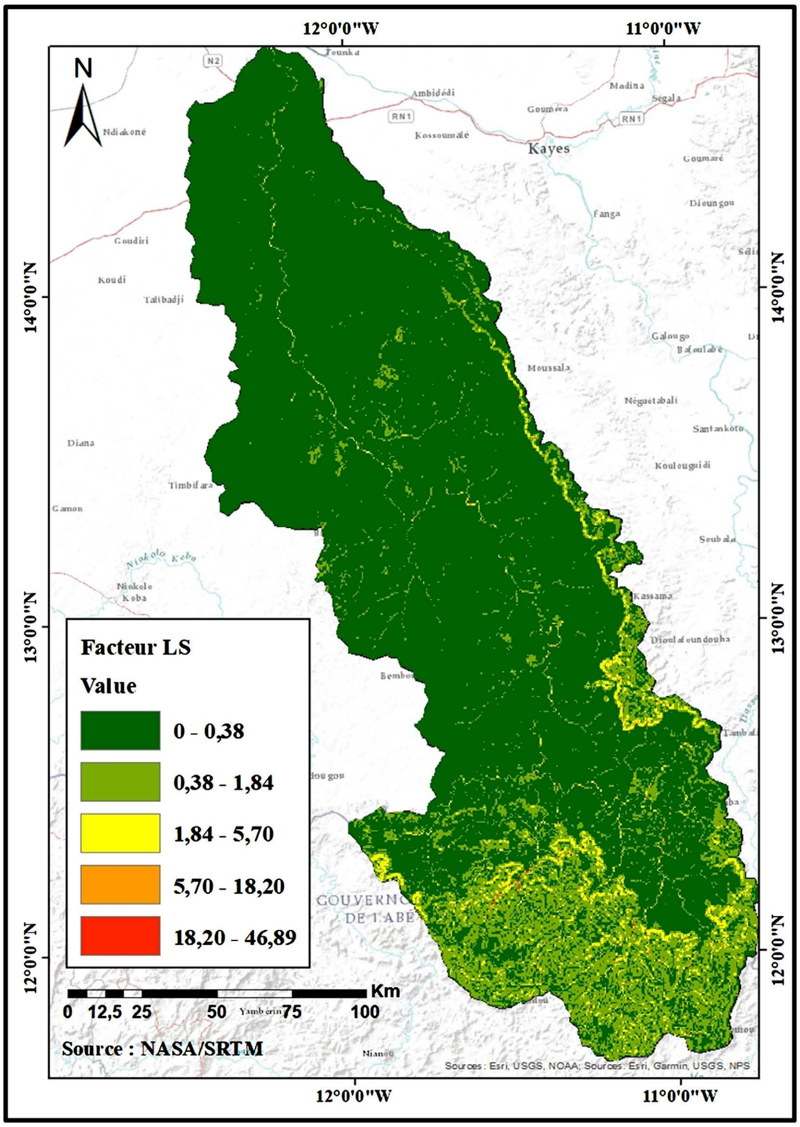

Figure 6. Topographic factor in the Falémé sub-basin.

Vegetation Cover and Anti-erosion Practices (C and P Factors)

The analysis of vegetation cover and erosion control practices shows that the Falémé sub-basin is largely composed of bare land. Well-forested areas represent a very small portion, mainly in the southern part of the sub-basin, making the area more vulnerable to erosion. Erosion control practices are also underdeveloped, with most values ranging between 0.8 and 0.9, indicating a lack of such practices across most of the sub-basin (Figure 7).

4.1.2. Soil Loss Mapping (Combination of All Factors)

Soil loss in the Falémé sub-basin is primarily located in the southern and southeastern parts, as well as along the main watercourse. The majority of predicted losses are very low, with values below 6.7 t/ha/year for 80.12% of the basin. According to the FAO classification (Table 3), these losses are considered low to be tolerable.

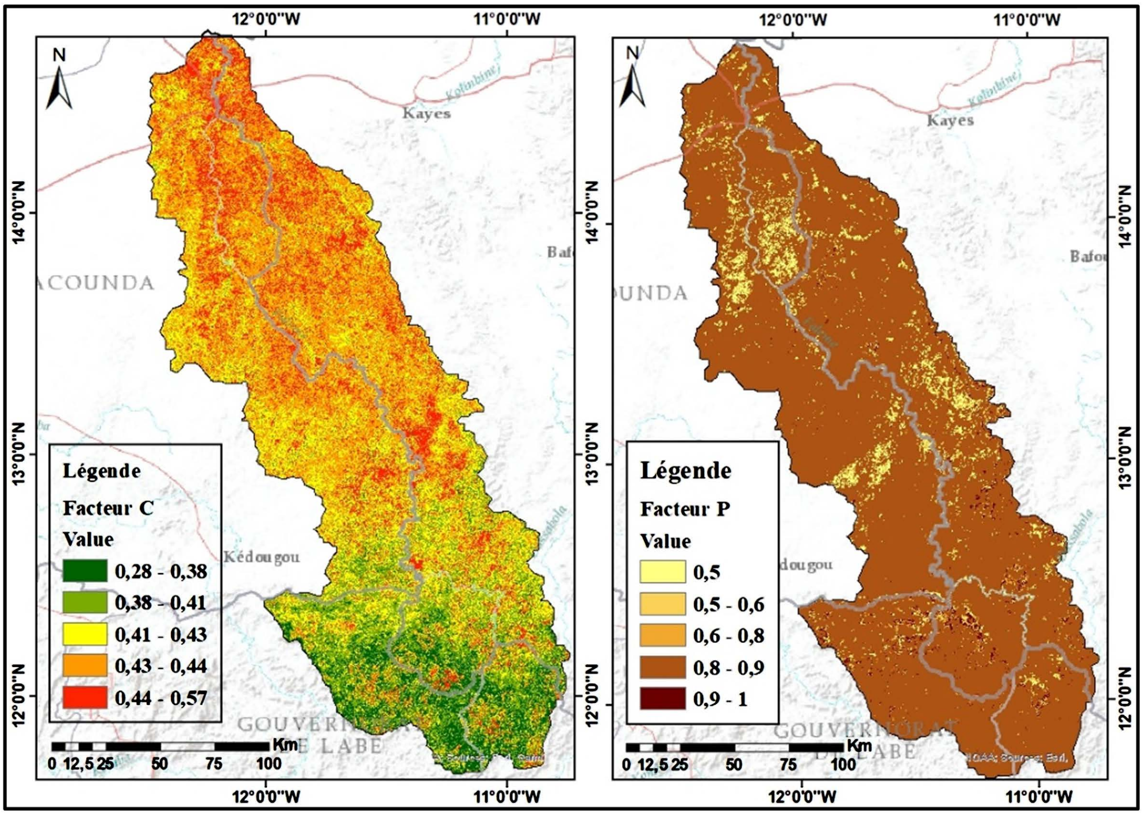

Figure 7. Map of vegetation cover and erosion control practices in the Falémé sub-basin.

Table 3. FAO soil loss classification [18].

Erosion Class	Soil Loss (t/ha/year)
Tolerable	<6.7
Low	6.7 - 11.2
Moderate	11.2 - 22.4
High	22.4 - 33.6
Severe	≥33.6

The combination of rainfall, topographic, pedological, anthropogenic, and vegetation cover factors led to the result shown in Figure 8.

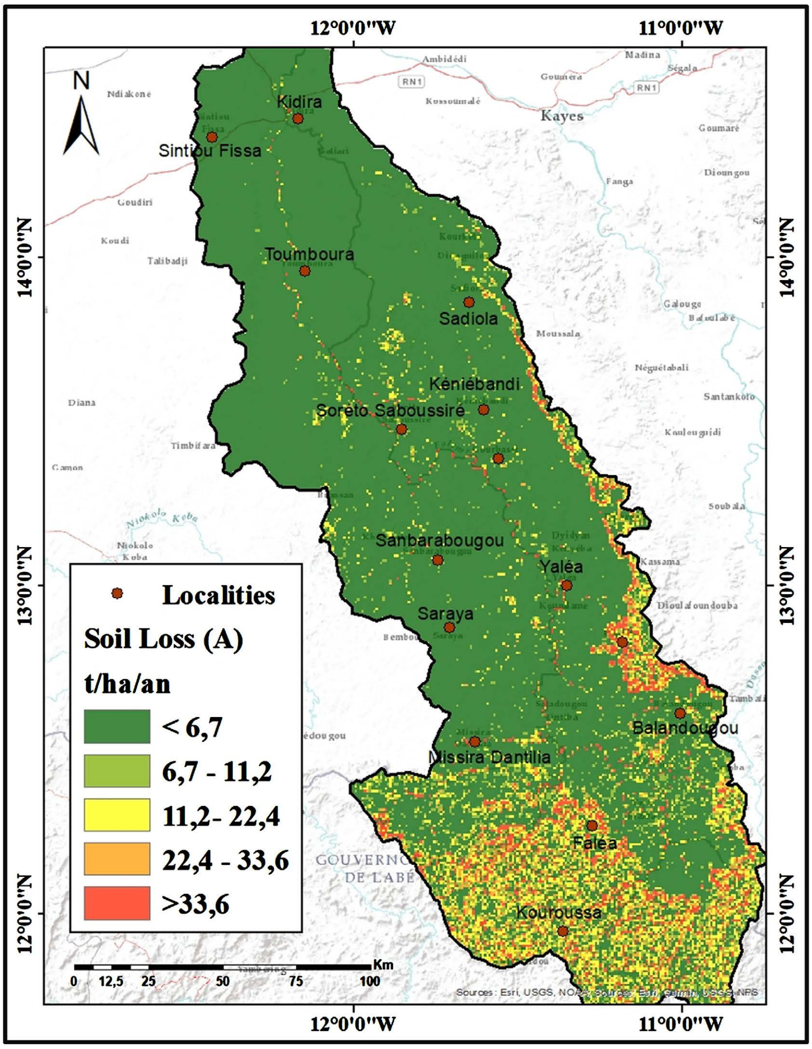

Figure 8. Annual soil loss map in the Falémé sub-basin.

An analysis of the results, based on FAO classification, shows that 85.8% of the sub-basin area affected by erosion is considered tolerable to low, while 14.02% records moderate, high, and severe annual loss rates (Figure 9). Severe losses, located in the southeast and along the main river course as previously mentioned, are estimated at over 33.6 t/ha/year. This is particularly concerning in areas with high elevation.

A correlation study of the various factors associated with annual soil losses was conducted to analyze the relationships between slope, flow accumulation, rainfall erosivity, soil erodibility, vegetation cover, erosion control practices, and the amount of soil loss per pixel (Figure 10). Pixel-by-pixel extraction revealed a significant correlation between LS, R, P, K, and C factors, with p-values less than or equal to 0.05, in line with the applied RUSLE model.

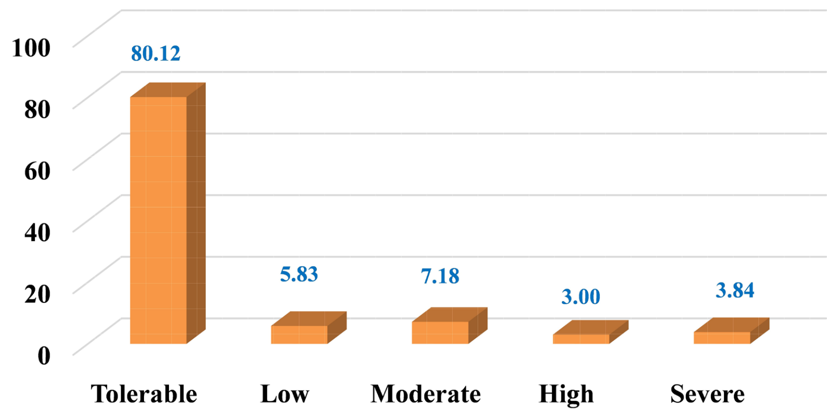

Figure 9. Percentage of recorded soil loss areas.

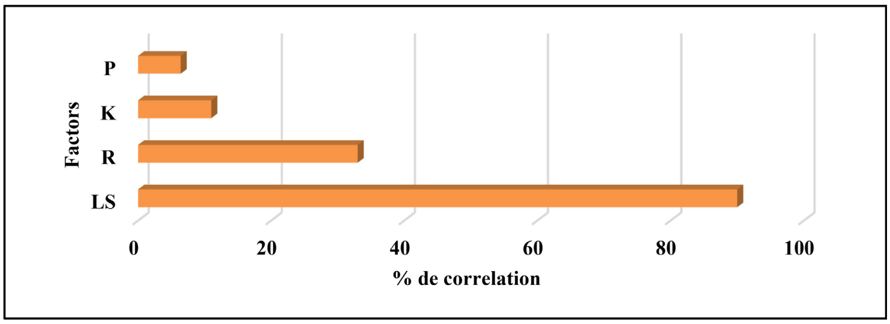

Figure 10. Correlation between A (soil loss) and influencing factors.

Flow accumulation, slope, and rainfall erosivity are the key parameters with the greatest influence on recorded soil losses. These variations, studied using a linear regression model, helped assess how each parameter contributes to increased soil loss. The results show that for each unit of the LS factor (slope length and steepness), soil loss increases by 20.51 units, explaining 80% of the soil loss variation highly significant. In contrast, the R factor accounts for 10.75%, the K factor 1.14%, and anti-erosion practices 0.41%. All these parameters, including the vegetation cover factor (C), are not sufficient on their own to explain the variations in soil loss. This demonstrates that soil loss is primarily influenced by the combined effect of all factors in the RUSLE model.

4.2. Discussion

4.2.1. Results of Soil Losses

Modeling water erosion using Earth observation products represents a significant advancement in understanding land degradation processes. It allows, through the application of empirical models, to provide answers that may open avenues for further research on soil degradation in watersheds. In this study, the use of Earth observation products combined with modeling methods enabled both qualitative and quantitative assessments of water induced soil erosion in the Falémé sub-basin. The qualitative study provided a better understanding of the physical characteristics of the basin and how they influence its behavior in response to soil erosion. The quantitative results based on the RUSLE model estimated annual soil loss to be below 6.7 t/ha/year for 80.12% of the basin area, which is considered highly tolerable according to the FAO classification [18]. However, although the erosion rate is mostly tolerable with in the sub-basin, around 14% of the area located in higher altitudes shows losses exceeding 11 t/ha/year beyond the tolerable limit for high altitude areas in tropical zones [19].

The estimated soil losses in the sub-basin, according to the RUSLE model, are higher than those reported by [4] in the Saraya area, which ranged from 0.01 to 134.64 t/ha/year. They also exceed the findings [19], who estimated losses above 200 t/ha/year in the Congo basin, a region with similar topographical characteristics. However, the variation in this study ranges from 0 to 298 t/ha/year across the sub-basin, reaching up to 723 t/ha/year on certain pixels. This could be attributed to overestimation issues, a known limitation in soil loss modeling [20]. Nevertheless, the results remain below those [21], who reported annual losses of 3487 t/ha/year on the Thies region.

4.2.2. Comparative Study of Other Sub-Basins

Soil loss modeling is also crucial in understanding the sediment dynamics of the broader Senegal River basin. It allows for the evaluation of sediment contributions from different sub-basins. This analysis provided in-depth insights into the erosive processes affecting the Senegal River basin.

The Falémé sub-basin connects with the Bafing, Bakoye, Baoulé, Kolimbiné, and Karakoro sub-basins before forming the main course of the Senegal River (**Figure 11**). All these sub-basins contribute to sediment yield, and their evaluation is essential in understanding water erosion in the Senegal River system.

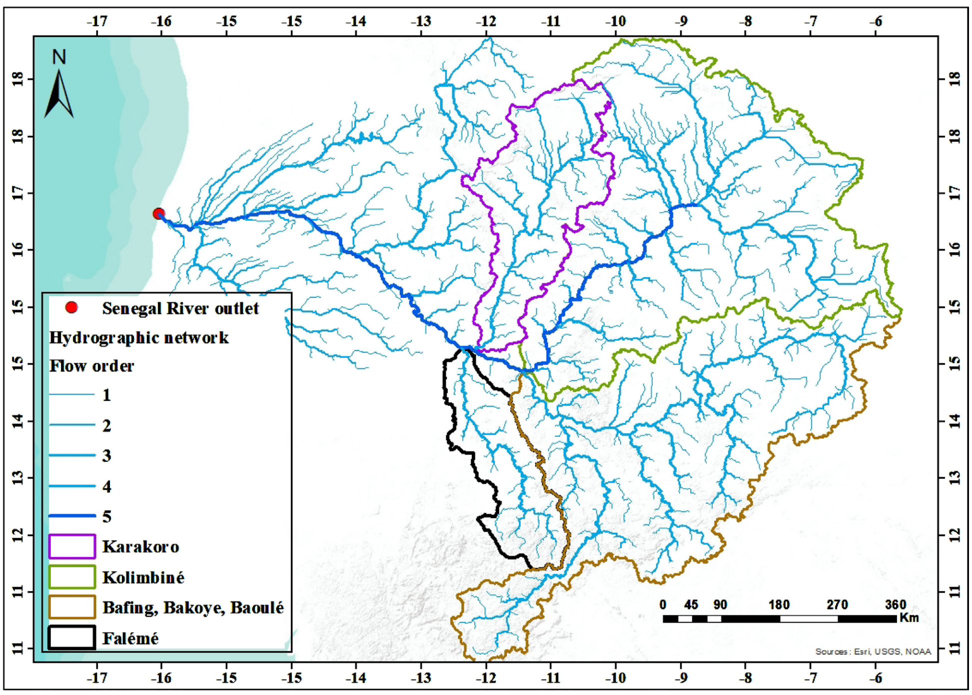

Figure 11. Other sub-basins connected to the Falémé sub-basin.

Based on the study results, for an area of 29927.82 km^2 representing about 5% of the Senegal River basin, the average soil loss in the Falémé sub-basin is estimated at 212.41 t/ha/year. In comparison:

- Bafing, Bakoye, and Baoulé sub-basins (25.8% of the basin area) average 390.9 t/ha/year,
- Kolimbiné: 293.5 t/ha/year (29% of the basin),
- Karakoro: 33.97 t/ha/year (8.5% of the basin).

Overall, soil losses are generally more significant in the south, particularly below the 1500 mm isohyet (Figure 12).

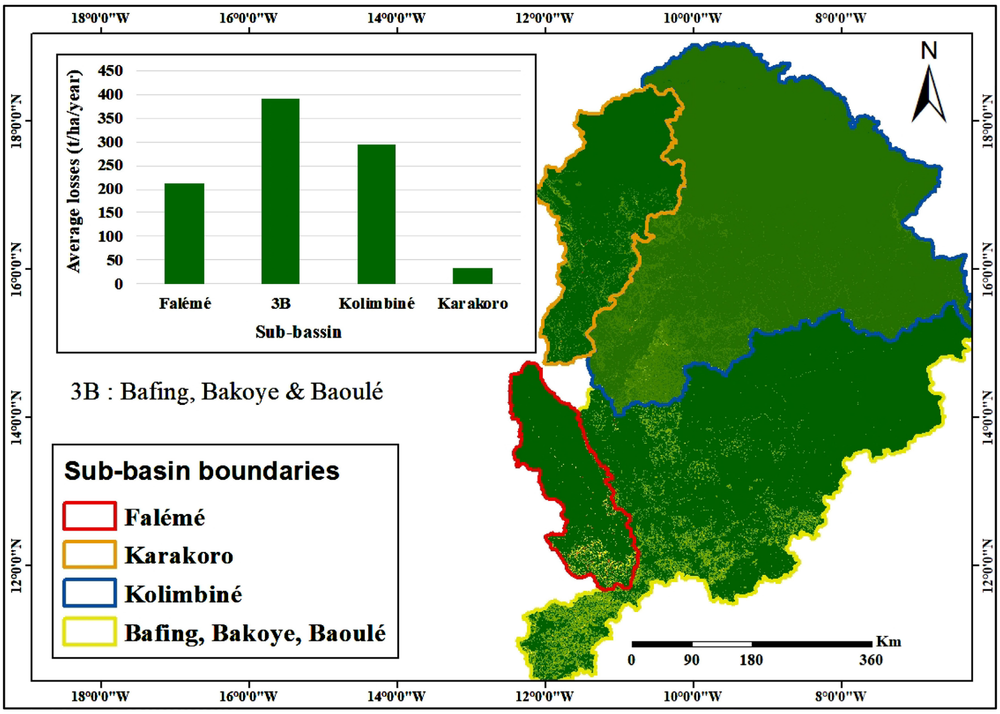

Figure 12. Average soil loss comparison with other sub-basins.

4.2.3. Limitations of the RUSLE Model

However, it is important to highlight the limitations of the RUSLE model, which must be considered when interpreting results.

Although widely used for predicting soil losses in African regions, RUSLE's applicability is subject to debate. Initially developed in the United States, the model has undergone several adaptations for different geographic contexts. However, applying its equations across vastly different regions can hinder its accuracy, as it relies heavily on local climatic conditions.

Calibration and the availability of certain types of data such as kinetic energy, rainfall intensity, and soil permeability pose challenges for many researchers [22]. Indeed, such data are not always available, particularly in many African countries. In this study, some parameters like rainfall intensity and energy were not included in the calculation of the rainfall erosivity factor, potentially impacting the accuracy of the results. The rainfall erosivity factor (R) was estimated using a normalized equation [11], which uses precipitation data. A maximum value of 827 MJ·mm/ha·h·year was obtained in the southern part of the basin.

[4] and [23] reported maximum R values of 637.85 MJ·mm/ha·h·year in the Kédougou area (central basin) and 4100 MJ·mm/ha·h·year in the Soungrougrou basin, respectively both with similar climatic conditions to Kédougou. The estimate is higher than the value obtained in this study, which was 650.79 MJ·mm/ha·h·year. The K factor for soil erodibility in this study ranged from 0.074 to 0.175 (t·ha·h/ha·MJ·mm), aligning closely [24] in West Africa and with [25], who found values between 0 and 0.12 in central Senegal. Differences in K values may also result from the use of different soil data sources such as the SOTER database. Given the dynamic nature of soil characteristics, periodic updates are recommended for more accurate analysis.

5. Conclusions

Water erosion remains a serious global issue, affecting large swaths of land. Considered the most severe form of erosion, it is the primary cause of soil degradation. This process has devastating effects on soil fertility, particularly in sub-Saharan Africa, where 83% of the population depends on land for their livelihood. The situation is worsened by climate change, traditional agricultural practices [26], and human activities that weaken the soil further, challenging food production security.

In the Falémé sub-basin, water erosion is mainly pluvial and influenced by several factors, including rainfall, soil type, topography, vegetation cover, and human activity. The interplay of these factors determines the level of vulnerability to erosion.

Located in an elongated sub-basin with increasing elevation from north to south, the Faleme sub-basin has favorable physical characteristics such as slower runoff in elongated basins. However, the southern part remains the most vulnerable to erosion, especially due to high precipitation exceeding 1000 mm/year, making it particularly prone to water erosion.

Acknowledgements

The listed authors contributed in various ways to the conception of this article. The site selection methodology was supervised by AN, the principal investigator. KMS handled data collection and processing, while EF and ML collaborated on statistical analyses and manuscript editing.

Conflicts of Interest

The authors declare that there is no conflict of interest.

References

[1] FAO (2015) "Etat des ressources en sol dans le monde" Organisation des Nations Unies pour l'alimentation et l'agriculture (FAO).

https://openknowledge.fao.org/items/36aab40e-0339-4394-b084-d4b638496622

[2] Chaaouan, J., Faleh, A., Sadiki, A. and Mesrar, H. (2014) Télédétection, SIG et modélisation de l'érosion hydrique dans le bassin versant de l'oued Amzaz, Rif Central. *Revue Française de Photogrammétrie et de Télédétection*, No. 203, 19-25. https://doi.org/10.52638/rfpt.2013.26

[3] Banque Mondiale (2009) Dégradation des terres au Sénégal. https://www.dapsa.gouv.sn/sites/default/files/publications/gdt.pdf

[4] Boissy, R., Ndiaye, M., Diatta, M. and Mbaye, M. (2022) Utilisation d'un SIG pour l'évaluation et la cartographie des risques d'érosion hydrique par l'Equation Universelle des Pertes en sol Révisée (RUSLE) dans le Département de Saraya (Sénégal). *VertigO*, **22**. http://journals.openedition.org/vertigo/38034%20;%20DOI%20:%20https://doi.org/10.4000/vertigo.38034

[5] Roose, E. (1994) Introduction à la gestion conservatoire de l'eau, de la biomasse et de la fertilité des sols (GCES). Bulletin pédologique de la FAO. https://www.fao.org/4/T1765F/T1765F00.htm

[6] Wischmeier, W.H. and Smith D.D. (1978) Predicting—Rainfall Erosion Losses, a Guide to Conservation Planning. Manuel agricole de l'USDA n° 537, Maryland. https://www.engr.colostate.edu/~pierre/ce_old/Projects/Paperspdf/Dawod-JulienII87.pdf

[7] Dubucq, M. (1986) Télédétection spatiale et Érosion des sols. Étude bibliographique. Laboratoire de Pédologie et de Géochimie, Université Paul Sabatier. https://horizon.documentation.ird.fr/exl-doc/pleins_textes/cahiers/PTP/24517.PDF

[8] Faye, C. (2016) Variabilité et tendances observées sur les débits moyens mensuels, saisonniers et annuels dans le bassin de la Falémé (Sénégal). *Hydrological Sciences Journal*, **62**, 259-269. https://doi.org/10.1080/02626667.2014.990967

[9] Rochette, C., Camus, H., Danuc, R. and Pereira, B.S. (1974) Le bassin du fleuve Sénégal. ORSTOM, 440. https://horizon.documentation.ird.fr/exl-doc/pleins_textes/pleins_textes_6/Mon_hydr/04347.pdf

[10] Roose, E. (1977) Erosion et ruissellement en Afrique de l'Ouest. Vingt années de mesures en petites parcelles. ORSTOM, Travaux et doc., n° 78, 105 p. https://horizon.documentation.ird.fr/exl-doc/pleins_textes/pleins_textes_6/Tra_d_cm/09011.pdf

[11] Nguyen, T.H. (1996) Identify the Factors Effect to Soil Erosion and Forecast Soil Erosion on Slope Land. Ph.D. Dissertation, Water Resources University of Vietnam.

[12] Arnoldus, H.M.J. (1980) An Approximation of the Rainfall Factor in the Universal Soil Loss Equation, Assessment of Erosion. FAO Land and Water Development Division, Wiley & Sons, 127-132.

[13] Pham, T.G., Degener, J. and Kappas, M. (2018) Integrated Universal Soil Loss Equation (USLE) and Geographical Information System (GIS) for Soil Erosion Estimation in a Sap Basin: Central Vietnam. *International Soil and Water Conservation Research*, **6**, 99-110. https://doi.org/10.1016/j.iswcr.2018.01.001

[14] Williams, J.R. (1995) The EPIC Model. In: Singh, V.P., Ed., *Computer Models of Watershed Hydrology*, Water Resources Publications, 909-1000.

[15] Julia, P. (2007) Estimation et spatialisation de l'érosion hydrique des sols en Nouvelle-Calédonie: Utilisation de l'équation universelle de perte de sol assistée d'un SIG sur les communes de Voh, Koné et Pouembout. Mémoire de master Sciences du territoire.

[16] Mitasova, H., Hofierka, J., Zlocha, M. and Iverson, L.R. (1996) Modelling Topographic Potential for Erosion and Deposition Using GIS. *International Journal of Geographical Information Systems*, **10**, 629-641. https://doi.org/10.1080/02693799608902101

[17] Bolline, A. (1982) Etude et prévision de l'érosion des sols limoneux cultivés en moyenne Belgique. Thèse Dr Géographie Université Liège.

[18] Dumas, P. (2010) Méthodologie de cartographie de la sensibilité des sols à l'érosion appliquée à la région de Dumbéa à Païta-Bouloupari (Nouvelle-Calédonie). *Cahiers d'Outre-Mer*, **63**, 567-584. https://doi.org/10.4000/com.6123

[19] Nacishali, J. (2020) Cartographie de l'érosion hydrique des sols et priorisation des mesures de conservation dans le territoire d'Uvira (République démocratique du Congo). *Vertigo*, **20**. https://doi.org/10.4000/vertigo.28888

[20] Kabirigi, M., Mugambi, S., Musana, B.S., Ngoga, G.T., Muhutu, J.C., Rutebuka, J. and Nabahungu, N.L. (2017) Estimation du risque d'érosion des sols, sa valorisation et ses implications économiques pour la production agricole dans la partie occidentale du Rwanda. *Journal de Biologie Expérimentale et de Sciences Agricoles*, **5**, 525-536. https://doi.org/10.18006/2017.5(4).525.536

[21] Diédhiou, A. and Lo, M.L. (2018) Modélisation de l'érosion hydrique des sols cultivés ou non du plateau de Thiès (Sénégal). *International Journal of Innovation and Applied Studies*, **25**, 210-221.

[22] Yameogo, A., Somé, Y.S.C., Palé, S. and Badaye, A.S. (2021) Application de SIG/RUSLE à l'estimation de l'érosion par ruissellement en nappe dans le bassin versant supérieur de la Sissili (Burkina Faso). *Geo-Eco-Trop*, **45**, 299-310.

[23] Faye, C., Diéye, S. and Fall, A. (2022) Impacts du changement d'utilisation des terres sur l'érosion hydrique des sols au Sénégal: Cas du bassin versant du Soungrougrou (Affluent du fleuve Casamance). *Revue Marocaine de la Géomorphologie*, No. 6, 60-68.

[24] Roose, E. and Sarrailh, J.M. (1989) Erodibilité de quelques sols tropicaux: Vingt années de mesure en parcelles d'érosion sous pluies naturelles. https://horizon.documentation.ird.fr/exl-doc/pleins_textes/cahiers/PTP/30456.PDF

[25] Ndao, C.T. (2022) Modélisation de l'érosion Hydrique des sols à l'aide des techniques RUSLE/SIG/Télédétection: Une étude de cas du bassin versant de Sokone dans le Delta du Saloum. Mémoire de master, École Nationale Supérieure d'Agriculture.

[26] Sané, B., Faye, C. and Sané, T. (2022) Evaluation de l'érosion hydrique des sols dans deux bassins versants non jaugés, Djibonker et Agnak, (Basse Casamance Méridionale, Sénégal). *Dynamiques Environnementales*, **49-50**, 128-156. https://doi.org/10.4000/dynenviron.7178